Energy LAB

2022, 1, 220005

Supporting Information

Interface engineering-inspired electron regulation in Pt/Pd hetero-metallene for methanol-assisted hydrogen evolution

Songliang Liu, Shuli Yin, Lin Cui, Hongjie Yu, Kai Deng, Ziqiang Wang, You Xu, Liang Wang, and Hongjing Wang*

State Key Laboratory Breeding Base of Green-Chemical Synthesis Technology, College of Chemical Engineering, Zhejiang University of Technology, Hangzhou 310014, P. R. China.

Corresponding author

*E-mail: hjw@zjut.edu.cn

Experimental Section

Materials Characterization

The morphology, structure and composition of the sample were characterized by scanning electron microscope (SEM) was conducted on a ZEISS Gemini 500 scanning electron microscope operating at 5 kV, transmission electron microscopy (TEM) was performed on a JEOL-2100F instrument equipped with energy dispersive X-ray spectroscopy, and X-ray diffraction (XRD) pattern was conducted on a PANalyticalX'Pert Powder with Cu Kα radiation X-ray source (λ = 0.154056 nm). The surface charge and surface chemical component of samples were investigated by X-ray photoelectron spectroscopy (XPS) measurements were conducted on a VG ESCALAB MK II instrument. AFM (MFP-3D Infinity, Asylum Research, USA) was used to determine the thickness of the nanosheets. A nuclear magnetic resonance (NMR) spectrometer was carried out on a Bruker Avance NEO 500.

Electrocatalytic Experiments

All electrochemical data were performed at a CHI660E electrochemical workstation via a two-electrode or three-electrode system (reference electrode: Ag/AgCl electrode, counter electrode: graphite rod) containing cyclic voltammetry (CV), linear sweep voltammetry (LSV), electrochemical impedance spectra (EIS), chronoamperometric (I-t) curves, chronopotentiometry(V-t) curves. In the case of three-electrode system for methanol oxidation reaction (MOR) and hydrogen evolution reaction (HER), the electrocatalyst ink was prepared by adding 2 mg of electrocatalyst into a 1 mL mixed solution containing 700 μL of water, 200 μL of isopropanol and 100 μL of Nafion (0.5 wt%). The

electrocatalyst ink (5 μL) was transferred onto a polished glassy carbon electrode (GCE, 3 mm in diameter) surface and dried at 50 °C in an oven to obtain a working electrode. For the two-electrode system, the carbon paper (CP) is applied as the positive and negative electrodes with an electrocatalyst loading of 1 mg cm^{-2} (Pt/Pd hetero-metallene/CP). All the LSV curves were recorded with 95% iR-compensation. EIS was performed in the range of 100 kHz to 100 mHz with the amplitude of 5 mV.

CO stripping: Electrochemically active surface area (ECSA) was obtained through CO stripping experiments. The CV was performed for 10 cycles in 1 M N_2-saturated KOH solution with a scan rate of 100 mV s^{-1} over a potential range of 0 to 1.2 V (vs. RHE). Then, by bubbling CO for 30 min, followed by bubbling N_2 for 30 min was used to remove the dissolved CO. Finally, CO stripping experiments were performed at a scan rate of 20 mV s^{-1} with a potential range of 0 to 1.2 V (vs. RHE). According to the following equation, the ECSA of various catalysts is calculated:

$$\mathrm{ECSA} = Q/(m\mathrm{C})$$

where Q is the charge in the oxidation region for the adsorbed CO, m is the loading of Pt and Pd metals, C (420 μC cm^{-2}) is the required charge of monolayer adsorption for CO on Pt and Pd surface.

Density Functional Theory (DFT): All the DFT computations were conducted adopting the Vienna Ab initio Simulation Package (VASP). The interactions of ion-electron were depicted using the projector augmented wave approach and the general gradient approximation in the Perdew-Burke-Ernzerhof (PBE) Form was applied.

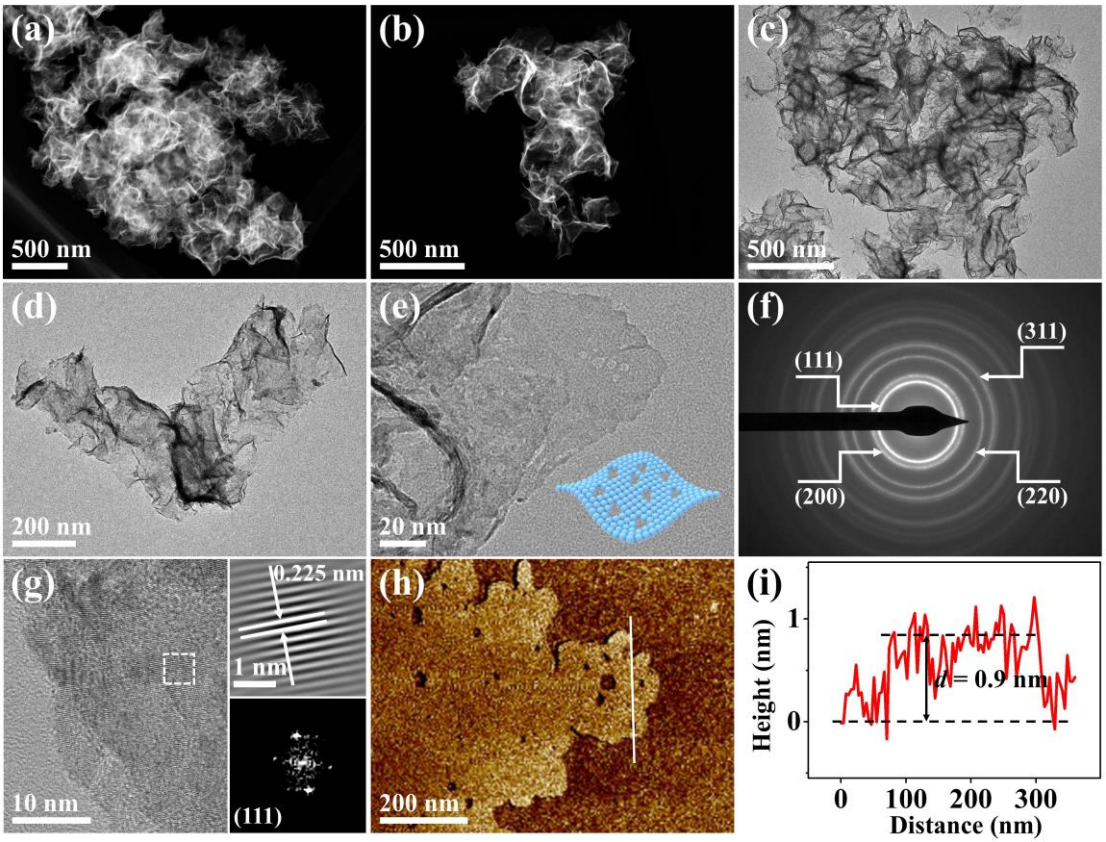

Figure. S1 (a and b) HAADF-STEM and (c-e) TEM images of the Pd metallene. (f) SAED and (g) HRTEM of the Pd metallene. (h) AFM image and corresponding (i) height profile. The insets in (g) display the lattice fringes of the square region and corresponding FFT pattern.

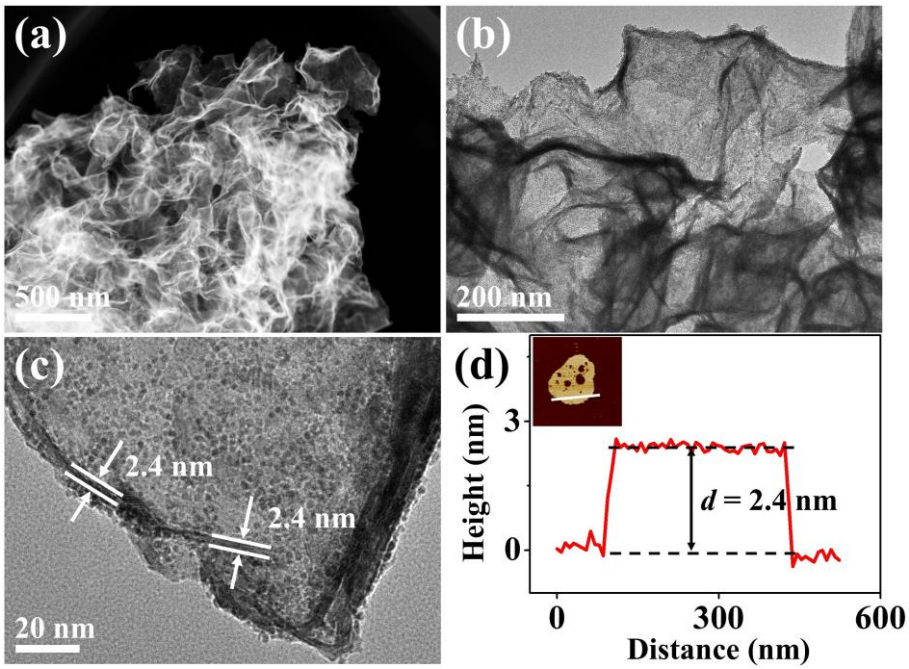

Figure. S2 (a) HAADF-STEM and (b and c) TEM images of the Pt/Pd hetero-metallene. (d) AFM image and corresponding height profile of the Pt/Pd hetero-metallene.

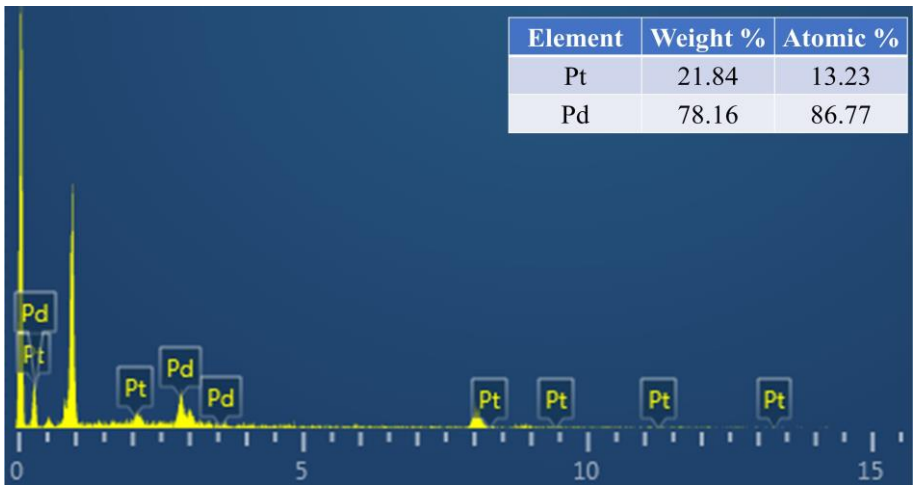

Figure. S3 EDX spectrum of the Pt/Pd hetero-metallene.

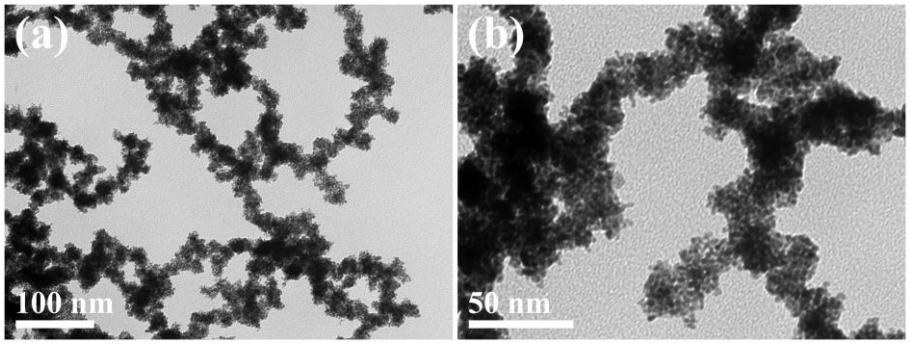

Figure. S4 TEM images of the samples prepared without add Pd metallene under the typical synthesis.

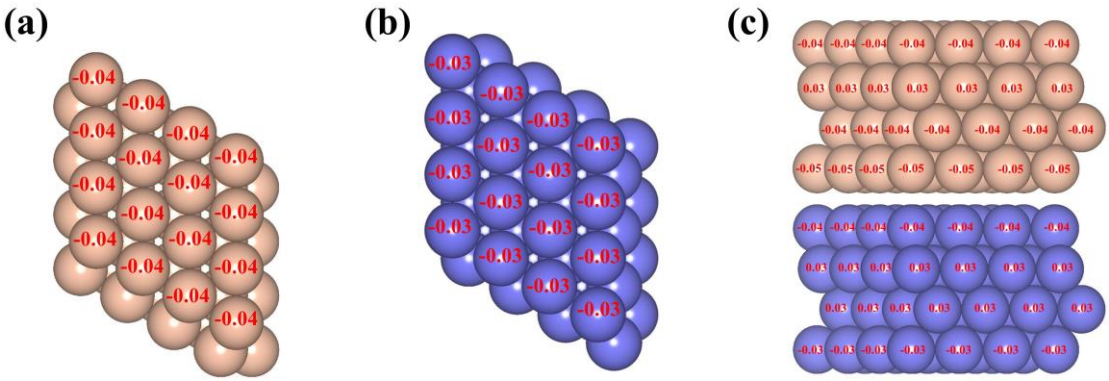

Figure. S5 Net charge obtained by Bader charge analysis marked on Pt and Pd atoms.

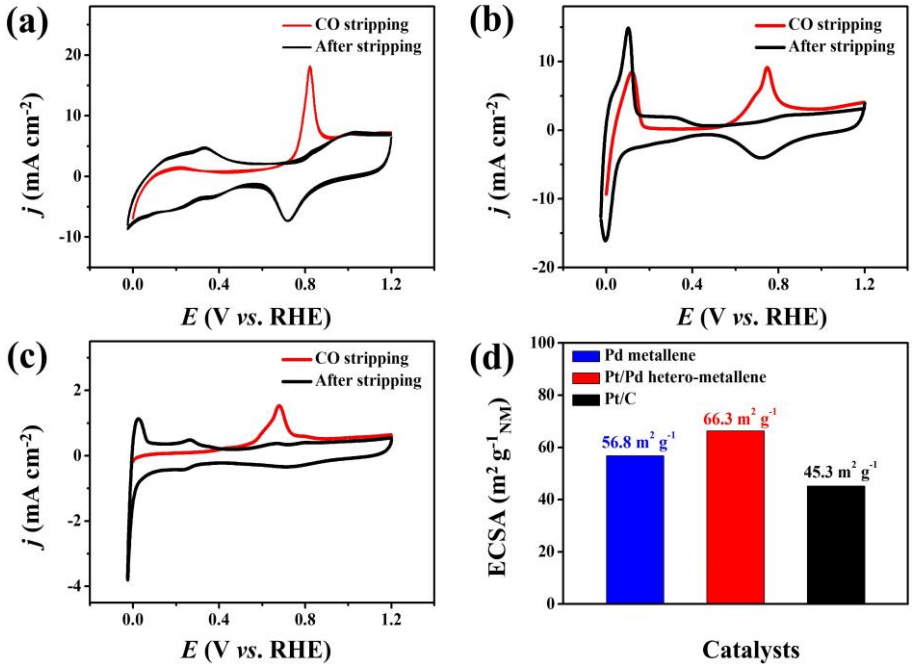

Figure. S6 CO stripping measurements of (a) Pd metallene, (b) Pt/Pd hetero-metallene and (c) Pt/C, in 1 M KOH at a scan rate of 20 mV s^{-1} and (d) the corresponding ECSA.

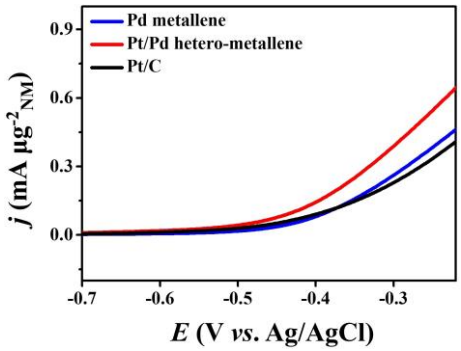

Figure. S7 LSV curves of various catalysts.

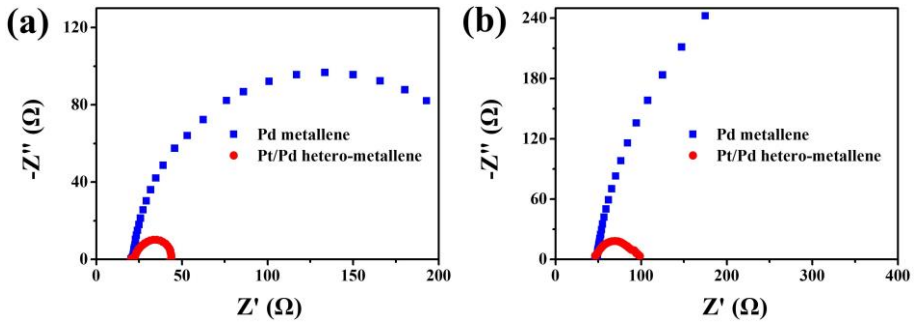

Figure. S8 EIS curves of Pt/Pd hetero-metallene and Pd metallene in 1 M KOH with and without 1 M CH_3OH under different applied potentials: (a) 1.0 V (*vs.* RHE) and (b) -0.2 V (*vs.* RHE).

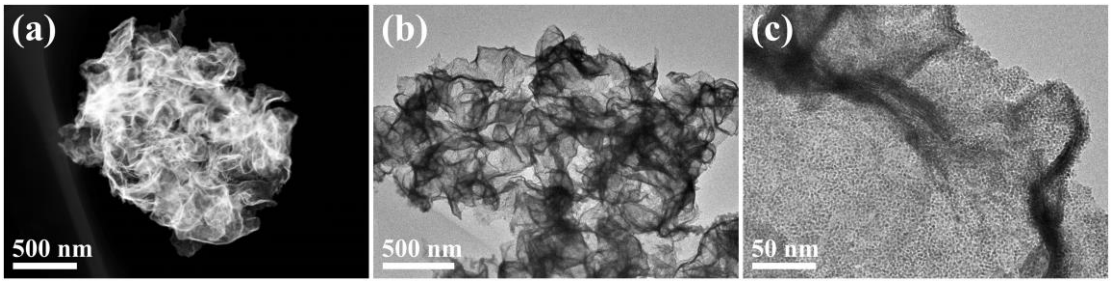

Figure. S9 HAADF-STEM and TEM images of the Pt/Pd hetero-metallene after the stability test.

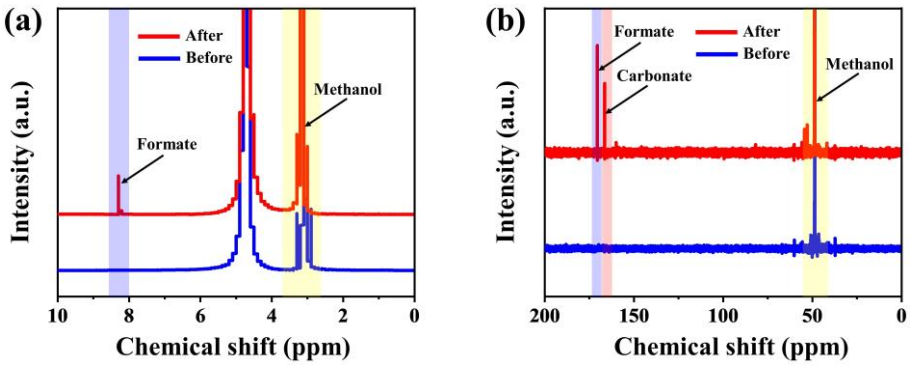

Figure. S10 (a) ^{1}H NMR and (b) ^{13}C NMR spectra of electrolyte before and after 15 h anodic MOR on Pt/Pd hetero-metallene electrode.

Table S1. The mass activity of Pt/Pd hetero-metallene compared with several recently reported MOR electrocatalysts.

Catalyst	Condition	Scan rate ($mV\ s^{-1}$)	Mass activity ($mA\ \mu g^{-1}_{NM}$)	Ref.
Pt/Pd hetero-metallene	**1 M KOH + 1 M CH_3OH**	**50**	**1.82**	**This work**
$Pt/Ni(OH)_2/rGO$	1 M KOH + 1 M CH_3OH	50	1.23	1
$Pt_{50}Pd_{50}$ SCs	1 M KOH + 1 M CH_3OH	50	0.33	2
$Pd_{30}Au_{70}/C$	1 M KOH + 1 M CH_3OH	50	0.95	3
PdNi NNs	1 M KOH + 1 M CH_3OH	50	1.11	4
Pd−Co J-NWs	1 M KOH + 1 M CH_3OH	50	1.21	5
Pd_1Cu_5	1 M KOH + 1 M CH_3OH	50	1.09	6
$Pd\text{-}CeO_2/SCS$	1 M KOH + 1 M CH_3OH	50	0.90	7
Pd-PdO PNTs	1 M KOH + 1 M CH_3OH	50	1.11	8

Table S2. The HER activity of Pt/Pd hetero-metallene compared with several recently reported catalysts in 1 M KOH.

Catalysts	Overpotential at 10 mA cm^{-2} (mV)	Electrolyte	Ref.
Pt/Pd hetero-metallene	**35**	**1 M KOH**	**This work**
PdIn bimetallene	171	1 M KOH	9
Pd/Ni-3	50	1 M KOH	10
Pd-nanodendrites/GNS	39.6	1 M KOH	11
PtNi-O/C	39.8	1 M KOH	12
Pd-Pt-S	71	1 M KOH	13
Pt_2Ni_3-P NWs	44	1 M KOH	14
PtPd@NLS	46	1 M KOH	15
15 min Pd/TiO_2	149	1 M KOH	16

Table S3. The cell voltage of Pt/Pd hetero-metallene/CP|| Pt/Pd hetero-metallene/CP methanol electrolyzer compared with several small molecule oxidation assisted water electrolysis.

Anode catalyst	**Cathode catalyst**	**Substrate molecule**	**Cell voltage (V)**	**Ref.**
Pt/Pd hetero-metallene	**Pt/Pd hetero-metallene**	**methanol**	**0.83**	**This work**
Pt-NP/NiO-NS	Pt-NP/NiO-NS	methanol	1.39	17
Co-Ni alloy	Co-Ni alloy	glucose	1.39	18
$Co(OH)_2$@HOS/CP	$Co(OH)_2$@HOS/CP	methanol	1.49	19
PdRh bimetallene	PdRh bimetallene	methanol	0.65	20
Ni_2P nanomeshes	Ni_2P nanomeshes	benzylamine	1.41	21
PdCu nanosheets	PdCu nanosheets	ethanol	0.7	22
NC/Ni-Mo-N/NF	NC/Ni-Mo-N/NF	glycerol	1.38	23
Pt nanocubes	Pt nanocubes	ammonia	0.68	24

References

[1] W. Huang, H. Wang, J. Zhou, J. Wang, P. N. Duchesne, D. Muir, P. Zhang, N. Han, F. Zhao, M. Zeng, J. Zhong, C. Jin, Y. Li, S. T. Lee, H. Dai, *Nat. Commun.,* 2015, *6*, 10035.

[2] L.-N. Zhou, X.-T. Zhang, Z.-H. Wang, S. Guo, Y.-J. Li, *Chem. Commun.,* 2016, *52*, 12737.

[3] Z. Yin, M. Chi, Q. Zhu, D. Ma, J. Sun, X. Bao, *J. Mater. Chem. A,* 2013, *1*, 9157.

[4] C. Zhu, D. Wen, M. Oschatz, M. Holzschuh, W. Liu, A. K. Herrmann, F. Simon, S. Kaskel, A. Eychmuller, *Small,* 2015, *11*, 1430.

[5] C. Wang, L. Zheng, R. Chang, L. Du, C. Zhu, D. Geng, D. Yang, *ACS Appl. Mater. Interfaces,* 2018, *10*, 29965.

[6] J. Sheng, J. Kang, H. Ye, J. Xie, B. Zhao, X.-Z. Fu, Y. Yu, R. Sun, C.-P. Wong, *J. Mater. Chem. A,* 2018, *6*, 3906.

[7] Q. Tan, C. Shu, J. Abbott, Q. Zhao, L. Liu, T. Qu, Y. Chen, H. Zhu, Y. Liu, G. Wu, *ACS Catal.,* 2019, *9*, 6362.

[8] T. J. Wang, F. M. Li, H. Huang, S. W. Yin, P. Chen, P. J. Jin, Y. Chen, *Adv. Funct. Mater.,* 2020, *30*, 2000534.

[9] S. Yin, S. Liu, Z. Wang, Y. Xu, X. Li, H. Wang, L. Wang, *Chem. Eng. J.,* 2022, *435*, 134711.

[10] M. Nie, Z. H. Xue, H. Sun, J. M. Liao, F. J. Xue, X. X. Wang, *Int. J. Hydrogen Energy,* 2020, *45*, 28870.

[11] L. Karuppasamy, L. Gurusamy, S. Anandan, C.-H. Liu, J. J. Wu, *Chem. Eng. J.,* 2021, *425*, 131526.

[12] Z. Zhao, H. Liu, W. Gao, W. Xue, Z. Liu, J. Huang, X. Pan, Y. Huang, *J. Am. Chem. Soc.,* 2018, *140*, 9046.

[13] J. Fan, K. Qi, L. Zhang, H. Zhang, S. Yu, X. Cui, *ACS Appl. Mater. Interfaces,* 2017, *9*, 18008.

[14] P. Wang, Q. Shao, J. Guo, L. Bu, X. Huang, *Chem. Mater.,* 2020, *32*, 3144.

[15] F. Wen, Y. Zhang, J. Tan, Z. Zhou, M. Zhu, S. Yin, H. Wang, *J. Electro. Chem.,* 2018, *822*, 10.

[16] M. Nie, H. Sun, J. Liao, Q. Li, Z. Xue, F. Xue, F. Liu, M. Wu, T. Gao, L. Teng, *Int. J. Hydrogen Energy,* 2021, *46*, 6441.

[17] G. Ma, X. Zhang, G. Zhou, X. Wang, *Chem. Eng. J.,* 2021, *411*, 128292.

[18] C. Lin, P. Zhang, S. Wang, Q. Zhou, B. Na, H. Li, J. Tian, Y. Zhang, C. Deng, L. Meng, J. Wu, C. Liu, J. Hu, L. Zhang, *J. Alloy. Comp.,* 2020, *823*, 153784.

[19] K. Xiang, D. Wu, X. Deng, M. Li, S. Chen, P. Hao, X. Guo, J. L. Luo, X. Z. Fu, *Adv. Funct. Mater.,* 2020, *30*, 1909610.

[20] Q. Mao, P. Wang, Z. Wang, Y. Xu, X. Li, L. Wang, H. Wang, *Applied Mater. Today*,

2022, *26*, 101400.

[21] Y. Ding, B.-Q. Miao, S.-N. Li, Y.-C. Jiang, Y.-Y. Liu, H.-C. Yao, Y. Chen, *Appl. Catal. B: Environ.,* 2020, *268*, 118393.

[22] X. Zhao, L. Dai, Q. Qin, F. Pei, C. Hu, N. Zheng, *Small* 2017, *13*, 1602970.

[23] Y. Xu, M. Liu, S. Wang, K. Ren, M. Wang, Z. Wang, X. Li, L. Wang, H. Wang, *Appl. Catal. B: Environ.,* 2021, *298*, 120493.

[24] H.-Y. Sun, G.-R. Xu, F.-M. Li, Q.-L. Hong, P.-J. Jin, P. Chen, Y. Chen, *J. Energy Chem.,* 2020, *47*, 234.